

Sl. No.	<p style="text-align: center;">IIT Ropar List of Recent Publications with Abstract Coverage: September, 2020</p>
1.	<p>A New Permanent Magnet Type Magnetorheological Finishing Tool for External Cylindrical Surfaces Having Different Outer Diameter AS Rana, TS Bedi, V Grover - Advances in Production and Industrial Engineering: Part of the Lecture Notes in Mechanical Engineering book series (LNME), 2020</p> <p>Abstract: An improved magnetorheological finishing process has been developed with three permanent magnets for nano finishing the external surface of cylindrical workpieces. The cylindrical permanent magnets used in the developed tool are placed at an angle of 90° from each other. The three cylindrical permanent magnets are positioned in such a way that all three maintain an equal working gap with the surface of cylindrical workpiece. Finite Element (FE) analysis of the entire setup has also been performed in the Maxwell Ansoft V13 software to observe the dispersal of magnetic field density in the working gap. In the current study, the preliminary experimentations have been carried out to evaluate the finishing capability of the present developed tool. Experiments have been conducted over the external cylindrical workpiece made of copper which can be used as an electron discharge machining (EDM) electrode. After the experimentations of 45 min over the entire cylindrical workpiece made of copper, the average surface roughness Ra gets reduced from 224 to 67 nm with negligible surface defects which confirm the finishing performance of the developed finishing tool.</p>
2.	<p>A way forward towards the improvement of tensor force in pf-shell K Jha, P Kumar, S Sarkar, PK Raina, S Aydin - Nuclear Physics A, 2020</p> <p>Abstract: In many shell model interactions, the tensor force monopole matrix elements are observed to retain systematic trends originating in the bare tensor force. In this work, however, we note for GX-interactions of pf-shell that the seven out of ten $T = 1$ tensor force monopole matrix elements do not share these systematic. We ameliorate this disparity making use of Yukawa-type tensor force and spin-tensor decomposition. Furthermore, we have modified the single-particle energy of $1p_{3/2}$ orbit and two TBMEs of $0f$-orbit, and the revised interaction has been tested from Ca to Ge isotopes with various physics viewpoints. The results are found to be satisfactory with respect to the experimental data.</p>
3.	<p>Analysis of single-cell transcriptomes links enrichment of olfactory receptors with cancer cell differentiation status and prognosis S Kalra, A Mittal, K Gupta, V Singhal, A Gupta, T Mishra, S Naidu... - Communications Biology, 2020</p> <p>Abstract: Ectopically expressed olfactory receptors (ORs) have been linked with multiple clinically-relevant physiological processes. Previously used tissue-level expression estimation largely shadowed the potential role of ORs due to their overall low expression levels. Even after the introduction of the single-cell transcriptomics, a comprehensive delineation of expression dynamics of ORs in tumors remained unexplored. Our targeted investigation into single malignant cells revealed a complex landscape of combinatorial OR expression events. We observed differentiation-dependent decline in expressed OR counts per cell as well as their expression intensities in malignant cells. Further, we constructed expression signatures based on a large spectrum of ORs and tracked their enrichment in bulk expression profiles of tumor samples from The Cancer Genome Atlas (TCGA). TCGA tumor samples stratified based on OR-centric signatures exhibited divergent survival probabilities. In summary, our comprehensive</p>

	analysis positions ORs at the cross-road of tumor cell differentiation status and cancer prognosis.
4.	<p>Analytical Steady-State Solution for a Three-Dimensional Partially Penetrating Ditch Drainage System Receiving Water from an Uneven Ponding Field R Sarmah, AH Gazi - <i>Journal of Irrigation and Drainage Engineering</i>, 2020</p> <p>Abstract: A steady-state analytical solution is proposed for computing three-dimensional seepage into a partially penetrating ditch drainage system receiving water from an uneven ponding field of finite size. The draining soil is assumed to be saturated, homogeneous, and anisotropic, resting on an impervious stratum. The correctness of the proposed model was checked with the analytical and experimental results for a simplified case. A numerical comparison was also carried out between the proposed analytical model and the corresponding finite-difference model for a given flow condition. The study highlights the significance of drain width, penetration depth, ponding distribution, and anisotropic ratio on the discharge distribution from the side and bottom face of the drains. In ditches of shallow depth, a significant rise in the percentage of bottom flow was found in soil with a low anisotropic ratio. With the introduction of the uneven ponding field, considerable enhancement in the contribution of flow discharge from the bottom face of the drain was observed. Travel time and orientation of flow paths were found sensitive to the point of release at the soil surface. Moreover, partially penetrating ditches promote a highly curved flow path from the surface to the recipient drain which in turn increases the travel time of the water particle.</p>
5.	<p>Anatomical variations in cortical bone surface permeability: Tibia versus femur R Kumar, AK Tiwari, D Tripathi, RP Main, N Kumar, P Sihota... - <i>Journal of the Mechanical Behavior of Biomedical Materials</i>, 2020</p> <p>Abstract: Cortical bone surfaces (periosteal and endosteal) exhibit differential (re)modelling response to mechanical loading. This poses a serious challenge in establishing an in silico model to predict site-specific new bone formation as a function of mechanical stimulus. In this regard, mechanical loading-induced fluid motion in lacunar-canalicular system (LCS) is assumed osteogenic. Micro-architectural properties, especially permeability regulate canalicular fluid motion within the bone. The knowledge of these properties is required to compute flow distribution. Along the same line, it is possible that cortical surfaces may experience differential fluid distribution due to anatomical variations in microarchitectural properties which may induce distinct new bone response at cortical surfaces. Nevertheless, these properties are not well reported for cortical surfaces in the literature. Accordingly, the present study aims to measure microarchitectural properties especially permeability at different anatomical locations (medial, lateral, anterior, and posterior) of periosteal and endosteal surfaces using nanoindentation. A standard poroelastic optimization technique was used to estimate permeability, shear modulus, and Poisson's ratio. The properties are also compared for two weight-bearing bones i.e. tibia and femur. Endosteal surface was found more permeable as compared to the periosteal surface. Tibial endosteal surface had shown greater permeability values at most of the anatomical locations as compared to femoral endosteal surface. The outcomes may be used to precisely predict site-specific osteogenesis in cortical bone as a function of canalicular flow distribution. This work may ultimately be beneficial in designing the loading parameters to stimulate desired new bone response for the prevention and the cure of bone loss.</p>

6.	<p>Anticipating the novel coronavirus disease (COVID-19) pandemic T Kaur, S Sarkar, S Chowdhury, SK Sinha, MK Jolly, PS Dutta - <i>Frontiers in Public Health</i>, 2020</p> <p>Abstract: The infectious novel coronavirus disease COVID-19 outbreak has been declared as a public health emergency of international concern, and later as an epidemic. To date, this outbreak has infected more than one million people and killed over fifty thousand people across the world. In most countries, the COVID-19 incidence curve rises sharply in a short span of time, suggesting a transition from a disease free (or low-burden disease) equilibrium state to a sustained infected (or high-burden disease) state. Such a transition from one stable state to another state in a relatively short span of time is often termed as a critical transition. Critical transitions can be, in general, successfully forecasted using many statistical measures such as return rate, variance and lag-1 autocorrelation. Here, we report an empirical test of this forecasting on the COVID-19 data sets for nine countries including India, China and the United States. For most of the data sets, an increase in autocorrelation and a decrease in return rate predict the onset of a critical transition. Our analysis suggests two key features in predicting the COVID-19 incidence curve for a specific country: a) the timing of strict social distancing and/or lockdown interventions implemented, and b) the fraction of a nation's population being affected by COVID-19 at the time of implementation of these interventions. Further, using satellite data of nitrogen dioxide which is emitted predominantly as a result of anthropogenic activities, as an indicator of lockdown policy, we find that in countries where the lockdown was implemented early and strictly have been successful in reducing the extent of transmission of the virus. These results hold important implications for designing effective strategies to control the spread of infectious pandemics.</p>
7.	<p>Automatic Prediction of Group Cohesiveness in Images S Ghosh, A Dhall, N Sebe, T Gedeon - <i>IEEE Transactions on Affective Computing</i>, 2020</p> <p>Abstract: This paper discusses the prediction of cohesiveness of a group of people in images. The cohesiveness of a group is an essential indicator of the emotional state, structure and success of a group of people. We study the factors that influence the perception of group-level cohesion and propose methods for estimating the human-perceived cohesion on the group cohesiveness scale. To identify the visual cues (attributes) for cohesion, we conducted a user survey. Image analysis is performed at a group-level via a multi-task convolutional neural network. For analyzing the contribution of facial expressions of the group members for predicting the Group Cohesion Score (GCS), a capsule network is explored. We add GCS to the Group Affect database and propose the 'GAF-Cohesion database'. The proposed model performs well on the database and can achieve near human-level performance in predicting a group's cohesion score. It is interesting to note that group cohesion as an attribute, when jointly trained for group-level emotion prediction, helps in increasing the performance for the later task. This suggests that group-level emotion and cohesion are correlated. Further, we investigate the effect of face-level similarity, body pose and subset of group on the task of automatic cohesion perception.</p>
8.	<p>Complexity and Algorithms for Semipaired Domination in Graphs MA Henning, A Pandey, V Tripathi - <i>International Workshop on Combinatorial Algorithms: Part of the Lecture Notes in Computer Science book series (LNCS, volume 11638)</i>, 2019</p> <p>Abstract: For a graph $G=(V,E)$ with no isolated vertices, a set $D\subseteq V$ is called a semipaired dominating set of G if (i) D is a dominating set of G, and (ii) D can be partitioned into two element subsets such that the vertices in each two element set are at distance at most</p>

	<p>two. The minimum cardinality of a semipaired dominating set of G is called the semipaired domination number of G, and is denoted by $\gamma_{pr2}(G)$. The MINIMUM SEMIPAIED DOMINATION problem is to find a semipaired dominating set of G of cardinality $\gamma_{pr2}(G)$. In this paper, we initiate the algorithmic study of the MINIMUM SEMIPAIED DOMINATION problem. We show that the decision version of the MINIMUM SEMIPAIED DOMINATION problem is NP-complete for bipartite graphs and chordal graphs. On the positive side, we present a linear-time algorithm to compute a minimum cardinality semipaired dominating set of interval graphs. We also propose a $(1+\ln(2\Delta+2))^{1+\ln(\frac{2\Delta+2}{\epsilon})}$-approximation algorithm for the MINIMUM SEMIPAIED DOMINATION problem, where Δ denotes the maximum degree of the graph and show that the MINIMUM SEMIPAIED DOMINATION problem cannot be approximated within $(1-\epsilon)\ln V /(1-\epsilon)\ln(\frac{2\Delta+2}{\epsilon}) V$ for any $\epsilon > 0$ unless $P = NP$.</p>
9.	<p>Cone type majorization and its strong linear preservers GSR Kosuru, S Saha - The Electronic Journal of Linear Algebra, 2020</p> <p>Abstract: This study introduces a novel notion, cone type majorization and characterizes the same. Further, the structure of linear preservers and strong linear preservers of this cone type majorization have been studied.</p>
10.	<p>Deep Learning based fully automatic efficient Burn Severity Estimators for better Burn Diagnosis J Chauhan, P Goyal - International Joint Conference on Neural Networks (IJCNN), 2020</p> <p>Abstract: Each year, burn injuries lead to several deaths and lifelong disabilities for many others. Timely provided appropriate diagnosis and treatment can reduce sufferings for many, however automated burns diagnosis techniques are still under exploration. Laser Doppler Imaging (LDI) has been found as promising for burns depth assessment, but high costs, delays and portability issues limit its usage in developing automated burns diagnosis methods. The visual images based automated approaches for burn diagnosis have been limitedly explored. This research presents a deep learning based novel approach for burn severity assessment and a new labeled dataset of burn images with varying burn severity that would be made publically available in order to facilitate and advance research for burn severity estimation. As skin characteristics vary across different body regions so will be the burn impact, so we propose customized burn severity estimators (specific to body parts) instead of having a single generic burn severity estimator for the whole human body. Extensive experiments were conducted to evaluate the performance of the proposed approach with different network settings, obtaining competitive results to state-of-the-art methods, despite each customized estimator using a smaller set of images compared to generic one. Also, the experiments suggest that the deep learning based customized estimators perform better than handcrafted features based methods for burns diagnosis.</p>
11.	<p>Directional ablation in radiofrequency ablation using a multi-tine electrode functioning in multipolar mode: an in-silico study using a finite set of states M Dhiman, AK Kumawat, R Repaka - Computers in Biology and Medicine, 2020</p> <p>Abstract: Purpose To analyse the feasibility of directional ablation using a multi-tine electrode. Methods A multi-tine electrode capable of operating in multipolar mode has been used to study the</p>

	<p>directional ablation. In addition to the basic design, similar to commercially available FDA approved multi-tine electrode, tines have been insulated from each other inside the probe base and tip using a thin insulating material of thickness 0.25 mm. A cylindrical single-compartment model of size 6 cm × 6 cm has been used to model normal liver tissue. The temperature-controlled radiofrequency ablation has been employed to maintain the tine-tips at different temperatures. Electro-thermal simulations have been performed by using a commercial multi-physics software package based on finite element methods. To make this study feasible a new approach to predict the ablations have been proposed and used in this study.</p> <p>Results</p> <p>Asymmetric ablation zone with up to 5 mm difference in ablation boundary between the intended and non-intended direction has been observed along the transverse direction. Reduction in ablation up to 5 mm along the axial direction in comparison to the monopolar mode has also been observed.</p> <p>Conclusion</p> <p>Multi-tine electrode modified to operate in multipolar mode can create directional ablations of different shapes and can be used to target position and shape specific tumours.</p>
12.	<p>Effect of Some Additives on Tribological Properties of SAE20W40 Lubricant HS Grewal, S Singh, H Singh, N Singh - Advances in Manufacturing Engineering, 2020</p> <p>Abstract: Friction and wear loss of various machining parts and pairs depend majorly on the quality of lubricants. Several types of additives are commercially used to enhance the tribological performance of a lubricant. In the present work, some novel lubricating liquids were prepared by mixing different additives, viz bromide, fluoride, iodide and acetate, in a commercial available SAE20W40 lubricant. Pin-on-disc investigations were performed to evaluate the effect of the prepared lubricants on wear rate and friction characteristics of mild steel and stainless steel sliding pair. Disc chamber was flooded with lubricants during testing. Fluoride was found to be the most successful additive to improve the performance of the given lubricant, whereas acetate as an additive made the base lubricant less efficient. It is believed that the strong bond stability of C–F bond during working conditions resulted in better performance of the lubricant after the addition of fluoride.</p>
13.	<p>Efficient Cache Resizing policy for DRAM-based LLCs in ChipMultiprocessors B Agarwalla, S Das, N Sahu - Journal of Systems Architecture, 2020</p> <p>Abstract: In today’s ChipMultiprocessors (CMPs), multiple cores share the common Last Level Cache (LLC), divided into multiple banks. As the data requirement is increasing the demand for larger LLC sizes is also increasing. The traditional SRAM technology is not area efficient to design such larger LLCs as demanded by the modern CMPs. From the last few years, DRAM technologies have been used to propose LLC. DRAM technology has almost 8 times density over the SRAM and hence larger cache size can be designed. Though DRAM is already considered as an alternative to design low cost, area-efficient larger size LLC, it must be used efficiently to get the benefits. Due to its overheads like access latency and refresh operations efficient techniques must be used to get better performance from DRAM LLC. In the existing works, it has been observed that though the larger LLC is required for the current as well as future data-intensive applications, the entire LLC may not be required while executing other applications. In such situations, some banks can be almost idle during a particular period of execution. These idle banks can be powered-off and restart later whenever required. The mechanism is called Cache Resizing as it resizes the cache (LLC) according to the current requirements. Cache resizing techniques are already proposed for SRAM based LLCs but due to</p>

	<p>the larger size of DRAM LLC, the same mechanisms cannot be used for DRAM LLCs. In this paper, we have proposed an efficient cache resizing policy for large sized LLC, especially for DRAM-based LLCs. We call our proposed cache resizing technique as Efficient Cache Resizing (ECR) which is implemented on top of a 3D Tiled CMP. Experimental analysis shows that ECR can reduce up to 44% more energy consumption as compared to the existing technique.</p>
14.	<p>Efficient hydrogenolysis of aryl ethers over Ce-MOF supported Pd NPs under mild conditions: mechanistic insight using density functional theoretical calculations AK Kar, SP Kaur, TJD Kumar, R Srivastava - Catalysis Science & Technology, 2020</p> <p>Abstract: Selective hydrogenolysis of lignin-derived aryl ethers under mild temperature and pressure conditions is an important milestone to be achieved to fulfill the future fuel demands from abundantly available biomass resources. Selective hydrogenolysis requires precise modulation of surface active sites of the catalyst to obtain the desired activity and selectivity. In this study, the selective hydrogenolysis of benzyl phenyl ether to phenol and toluene is achieved in methanol and water medium at a very low temperature and low H₂ pressure over a Pd nanoparticle decorated Ce-BTC metal–organic framework. The activity of the developed catalyst is two times higher than that of Pd decorated CeO₂. The structure–activity relationship is established using catalytic measurements, X-ray photoelectron spectroscopy, and transmission electron microscopy. The mechanistic insight into the hydrogenolysis of aryl ethers and the reasons behind the superior activity of Pd/Ce-BTC to that of Pd/CeO₂ are investigated using density functional theoretical (DFT) calculations. Spectroscopic measurements and DFT calculations suggest that the higher Pd⁰/Pd²⁺ ratio and higher adsorption of benzyl phenyl ether over Pd/Ce-BTC and the higher adsorption of phenol over Pd/CeO₂ are factors responsible for the higher activity of Pd/Ce-BTC than that of Pd/CeO₂. Efficient recyclability and hot filtration tests reveal that the catalyst exhibits no noteworthy loss in the activity after five consecutive cycles. The Pd/Ce-BTC catalyst displays a very high turnover frequency and low activation energy, which are very attractive from the industrial perspective and academic point of view.</p>
15.	<p>Energy-Efficient Strategy for Improving Coverage and Rate Using Hybrid Vehicular Networks D Saluja, R Singh, N Saluja, S Kumar - IEEE Transactions on Intelligent Transportation Systems, 2020</p> <p>Abstract: A decade back, emergency voice communication was the only target to support the patient in an ambulance. It is now evolved from emergency voice communication to vital signal monitoring and operating the machines from the remote place. This evolution requires support from technology to meet the high data rates along with reliability for the specified applications. The millimeter-wave (mmWave) communication support high data rate requirements of vehicular communication. However, in the case of mmWave, the radio signals vary fast. It poses the implementation challenge to the mmWave system in this scenario. The other implementations challenges of mmWave are high path loss, severe blockage and frequent beam updates which inhibit seamless connectivity (reliability) to vehicular nodes. However, the reliability is always a prime concern for any vehicular communication system. This paper addresses these challenges by implementing a novel energy-efficient strategy based on RSUs deployment and radio access technology (RAT). The strategy is to deploy RSUs on either side of the road and use an optimal combination of mmWave and microwave RAT. The essential analysis of such a hybrid system involves the evaluation of parameters based on the analytic model. Hence, this paper analytically obtains the expression for seamless coverage and connectivity. The analysis is also extended to rate and energy efficiency calculations. The analysis is supported by probabilistic models-based simulations that agree closely with</p>

	<p>computation results. The results claim that the proposed model leads to improved performance in terms of coverage and rate while maintaining the cost and energy efficiency within the limits.</p>
16.	<p>Experimental and Analytical Investigation of Poned Ditch Drainage System with Temporal Boundaries R Sarmah, G Barua, SA Kartha - Journal of Hydrologic Engineering, 2020</p> <p>Abstract: An analytical solution is proposed for a two-dimensional, fully-penetrating ditch drainage system by considering the boundaries at the ditch face and at the soil surface to change with time. The general assumption of instantaneous boundary impositions at the ditch face and at the surface of the soil is replaced by continuous time-varying boundary impositions at these faces, as they are expected to be more realistic and readily realized in actual field situations, as compared to static and instantaneous boundaries at the ditches and at the surface of the soil. However, the proposed analytical model is a versatile one, capable of tackling both instantaneous and continuous boundary impositions alike. To ascertain the validity of the solution, a few experiments on them have also been carried out. Further, the correctness of the proposed model is also checked for a simplified flow scenario by comparing it with an existing analytical solution to the problem. The study highlights that with the imposition of time-dependent boundaries, the maximum top discharge value gets reduced by multiple folds as compared to ponded drainage situations in which boundaries have been instantaneously imposed. It is also observed that the time taken by a ponded drainage system to reach a steady-state has a direct correlation with the time required to create steady water depths at the different boundaries of the problem. Further, the pathline and travel time of water particles are both found to be sensitive to the nature and distribution of the time-dependent boundaries of the problem.</p>
17.	<p>First Principle Analysis of Os-passivated Armchair Graphene Nanoribbons for Nanoscale Interconnects VK Nishad, AK Nishad, S Roy, BK Kaushik, R Sharma - IEEE 20th International Conference on Nanotechnology (IEEE-NANO), 2020</p> <p>Abstract: In this paper, transport properties of Osmium (Os)-passivated armchair graphene nanoribbons (AGNRs) have been explored for applications in nanoscale interconnects. Os has been used for passivation in place of Hydrogen (H). In general, H-passivation is used to reduce the edge scattering in AGNRs. However, this increases the bandgap of the structure. In our study, it is found that Os-passivation reduces the edge scattering with improvement in metallicity of AGNRs, which makes it suitable for future nanoscale interconnects. We have extracted key parameters, such as transmission spectrum, I-V characteristics, number of conduction channels, Fermi velocity, kinetic inductance and quantum capacitance. We have compared our results with Fe-passivated AGNRs. In case of Os-passivated AGNRs, up to eight conduction channels are seen that result in higher currents of up to 4x as compared to Fe-passivated AGNRs.</p>
18.	<p>Fission and Quasi-Fission in Reactions with Deformed Nuclei YM Itkis, AV Karpov, GN Knyazheva, EM Kozulin...PP Singh - Bulletin of the Russian Academy of Sciences: Physics, 2020</p> <p>Abstract: The mass-energy distributions of fragments formed in reactions $^{16,18}\text{O} + ^{232}\text{Th}$, ^{238}U, and $^{22}\text{Ne} + ^{232}\text{Th}$, ^{238}U at energies near the Coulomb barrier are measured to study the role of multimodal fission in the reactions of light ions with strongly deformed actinide nuclei. It is found that at these energies, multimodal fission affects significantly the mass-energy and angular distributions of fragments that results in an increase of the width of mass distributions and large angular anisotropy as in the case of quasifission.</p>

19.	<p>Improved exergy evaluation of ammonia-water absorption refrigeration system using inverse method A Singh, R Das - Journal of Energy Resources Technology, 2020</p> <p>Abstract: In this study, the compatibility of exergy destruction minimization (EDM) as the main objective is checked by plotting coefficient of performance (COP), exergy coefficient of performance (ECOP), and overall exergy destruction rate by simultaneously varying input operating temperatures for a 28 TR cooling load absorption system. The component-wise variation in exergy destruction is also considered and it is found that the maxima of COP and ECOP, and the minima of overall exergy destruction lies on a common point, and when the variation of operating temperatures is further extended, the exergy destruction in one of the component becomes negative, which marks the upper bound of the present analysis. At highest valid generator temperature (155 °C), the minimum possible overall exergy destruction rate is 53.50 kW and maximum COP is 0.523. Through inverse optimization (IO) using dragonfly algorithm (DA), the same overall exergy destruction rate is achieved for a wide range of generator temperatures much below than 155 °C, and as low as 127.34 °C. The above variation is explained in terms of flow ratio, mass flowrate of steam, and mass flowrate of cooling water.</p>
20.	<p>Inferring Location Types With Geo-Social-Temporal Pattern Mining T Anwar, K Liao, A Goyal, T Sellis, ASM Kayes, H Shen - IEEE Access, 2020</p> <p>Abstract: With a rapid growth in the global population, the modern world is undergoing a rapid expansion of residential areas, especially in urban centres. This continuously demands for increased general services and basic amenities, which are required according to the kind of population associated with the places. The advent of location-based online social networks (LBSNs) has made it much easier to collect voluminous data about users in different locations or spatial regions. The problem of mining location types from the LBSN data is largely unexplored. In this paper, we propose a pattern mining approach, using the geo-socialtemporal data collected from LBSNs, to infer types of different locations. The proposed method first mines frequent co-located users and user components from an LBSN and then performs a temporal pattern analysis to finally categorize the locations. Extensive experiments are conducted on two real datasets that demonstrate the efficacy of the proposed method in terms of mean reciprocal rank (MRR), visualisations, and insights. The resulting inference mechanism would be very useful in several application domains including urban planning, billboard placement, tour planning, and geo-social event planning.</p>
21.	<p>Influence of fuel injection pressure and injection timing on nanoparticle emission in light-duty gasoline/diesel RCCI engine MR Saxena, RK Maurya - Particulate Science and Technology, 2020</p> <p>Abstract: This work investigates the influence of fuel injection events on the nanoparticle emission characteristics of light-duty gasoline-diesel RCCI engine. The formation of nanoparticle emissions strongly depends on fuel injection events. The present study experimentally investigates the influence of diesel injection pressure, injection timing, and port-injected gasoline mass on the nanoparticles emitted from the gasoline-diesel RCCI engine. For this purpose, the engine is tested at different engine speeds and a fixed load of 1.5 bar BMEP without exhaust gas recirculation. The particle-size and number distribution (PSD) and total particle number (total PN) concentration are measured using a differential mobility spectrometer. The results depict that at higher diesel injection pressure (IP) operation, the peak of the NMP increases while the AMP peak decreases for neat diesel operation as well as RCCI engine.</p>

	<p>Nucleation, as well as accumulation mode particles, increases with advanced diesel injection timing in RCCI combustion. An increase in port fuel injected mass also leads to an increase in the total particle concentration and total unburned hydrocarbon (THC) emissions.</p>
22.	<p>Interaction of Cyanogen (NCCN) with Proton: A New Ab Initio Potential Energy Surface A Kushwaha, S Chhabra, TJD Kumar - Chemical Physics Letters, 2020</p> <p>Abstract: NCCNH⁺ is detected in interstellar medium recently. To characterize and study the collision dynamics, a new global potential energy surface for the NCCNH⁺ system has been generated using CCSD(T)/aug-cc-pVQZ method. NCCN-H⁺ has a large potential well of 7 eV indicating high stability of complex. The surface has been expanded in terms of Legendre polynomials. NCCN and NCCNH⁺ have been accurately characterized. The surface will be helpful for detailed understanding of quantum dynamics parameters such as ro-vibrational cross-sections and rate coefficients. The data obtained in this work will have perceptible impact to understand the cyanogen and protonated cyanogen chemistry in space.</p>
23.	<p>Investigations on probability of defect detection using differential filtering for pulse compression favourable frequency modulated thermal wave imaging for inspection of glass fibre reinforced polymers V Kher, R Mulaveesala, A Rani, V Arora - IOP SciNotes, 2020</p> <p>Abstract: Thermal Non-Destructive Testing and Evaluation (TNDT&E) plays a crucial role in industrial quality control and structural health monitoring of a variety of materials. Among various TNDT&E modalities, active Infrared Thermography (IRT) has emerged as an extremely promising approach and has gained enormous significance due to its quick, whole field, non-contact and quantitative defect detection capabilities. Pulse Compression favourable Thermal Wave Imaging (PCTWI) especially Frequency Modulated Thermal Wave Imaging (FMTWI) has become popular among a number of active IRT techniques because of increment in defect detection sensitivity as well as test resolution. The present work attempts to explore the applicability of differential filtering post processing scheme for pulse compression favourable FMTWI for enhanced detection contrast, resolution and Probability of Detection (PoD). The proposed scheme has been applied on a Glass Fibre Reinforced Polymer (GFRP) sample with sub-surface flat bottom hole (FBH) defects located inside the sample at different depths. The results presented clearly demonstrate that the differential contrast approach enhances the defect detection probabilities by considering maximum and minimum deviation dip values as a figure of merit. Hence, pulse compression favourable FMTWI employing differential filtering manifests higher Probability of Detection (PoD) for defects located at different depths as compared to taking into account the peak Correlation Coefficient(CC) as a statistical figure of merit. Further Probability of Detection (PoD) of the pulse compression favourable FMTWI technique has been improved by differential filtering post-processing based scheme that reduces the memory requirement, computational cost as well as complexity.</p>
24.	<p>Linear Algebraic Method of Solution for the Problem of Mitigation of Wave Energy Near Seashore by Trench-Type Bottom Topography A Kaur, SC Martha, A Chakrabarti - Journal of Engineering Mechanics, 2020</p> <p>Abstract: The problem involving mitigation of wave energy by trench-type structure, in particular, a pair of trenches imposed on the seabed in the absence and presence of a vertical wall, is examined for its solution. The problem under consideration leads to multiple series relations involving trigonometric functions. Instead of converting these relations into a system of integral equations, direct algebraic approaches are utilized for solving the reduced system of</p>

	<p>overdetermined algebraic equations and the corresponding solutions are obtained approximately. Here, the overdetermined system of algebraic equations are solved with the aid of the well-known least-squares (LS) and singular value decomposition (SVD) methods. Results involving the hydrodynamic quantities such as reflection and transmission coefficients related to the single trench problem are derived and are found to be in excellent agreement with the results available in the literature. The present algebraic methods appear to be very direct and quick. The energy balance relation for the given scattering problem is derived and used to check the accuracy of numerical results. Some important results such as the behavior of singularity in flow near each edge of the trenches, surface elevation profiles, and force experienced by the wall are investigated and analyzed through graphs to analyze the transformation of wave energy by a pair of trenches imposed on a seabed. It is observed that creation of a pair of trenches imposed on a seabed helps to reduce the wave load on the wall; consequently, the wall as well as the seashore (in absence of a wall) is protected.</p>
25.	<p>Multi-Partition Feature Alignment Network for Unsupervised Domain Adaptation S Sukhija, S Varadarajan, NC Krishnan, S Rai - <i>International Joint Conference on Neural Networks (IJCNN)</i>, 2020</p> <p>Abstract: In this paper, we present a novel unsupervised domain adaptation framework, Multi-Partition Feature Alignment Network, that learns a deep neural model for the target domain without the need for any supervision. Recent leading approaches for unsupervised domain adaptation are based on adversarial alignment. Aligning the global distribution of the domain representations via adversarial training does not guarantee the class-wise distribution alignment. The proposed approach is built on adversarial learning with the focus on carefully aligning class-wise domain representations. Our algorithm utilizes the pseudo-labels (the predicted labels) of the target features to stimulate class-wise alignment. As the pseudo-labels of individual target features can be erroneous, instead of iteratively aligning individual target samples, the proposed framework introduces a generic class-specific multi-partition alignment procedure that enables superior class-discriminative alignment of domain representations. The competitive performance of the proposed framework against state-of-the-art approaches over a wide variety of visual recognition tasks, namely, the digits classification task and the object recognition task, validates its effectiveness for unsupervised domain adaptation.</p>
26.	<p>Naphthalimide-gold-based nanocomposite for the ratiometric detection of okadaic acid in shellfish M Verma, M Chaudhary, A Singh, N Kaur, N Singh - <i>Journal of Materials Chemistry B</i>, 2020</p> <p>Abstract: Okadaic acid (OA) is one of the known marine biotoxins produced by various dinoflagellates and exists in seafood such as shellfish. The consumption of contaminated shellfish with OA leads to diarrhetic shellfish poisoning (DSP), which results in the inhibition of protein phosphatase enzymes in humans. This poisoning can cause immunotoxicity and tumor promotion due to the accumulation of okadaic acid in more than the allowed limit in bivalve molluscs. The reported methods for the detection of okadaic acid include mouse bioassays, immunoassays, chromatography coupled with spectroscopic techniques, electrochemical sensors and immunosensors. We have developed a naphthalimide-gold-based nanocomposite for the detection of okadaic acid. Individually, the organic nanoparticles (ONPs) of synthesized naphthalimide-based receptors and gold-coated ONPs are less sensitive for detection. However, fabrication of the composite of Au@ONPs and ONPs enhance the sensing properties and selectivity. The composite shows a ratiometric response in the UV-Vis absorption spectrum and quenching in the fluorescence profile with a detection limit of 20 nM for OA in aqueous</p>

	<p>medium. In cyclic voltammetry, a shift was observed in the cathodic peak (−0.532 V to −0.618 V) as well as in the anodic peak (−0.815 V to −0.847 V) with the addition of okadaic acid. To study the quick binding of the composite with OA, a time response experiment was performed. Also, the developed sensor retains its sensing ability in the pH range of 5–9 and in high salt conditions. Our developed composite can be used for the detection of OA in real applications.</p>
27.	<p>Noise-power-area optimised design procedure for OTAs with complementary input transistors for neural amplifiers DM Das, K Barot, A Srivastava, MS Baghini - IET Circuits, Devices & Systems, 2020</p> <p>Abstract: Simultaneous measurement of neural bio-potentials from a large number of neurons is finding applications in a diverse range of areas such as healthcare and brain-machine interfacing. Neural amplifiers used for these measurements have a tight specification of low-power, low-noise and small area. Most of the reported neural amplifiers use operational transconductance amplifier (OTA) based capacitive feedback amplifiers to meet these requirements. In this study, for the first time, a novel systematic noise-power-area optimised design procedure, for complementary input transistor based OTAs, used frequently in neural amplifiers is proposed. By applying the proposed design procedure, the authors have presented a neural amplifier design that is split into two stages to reduce area requirement and enhance linearity at the expense of slight degradation in noise efficiency factor. The presented design achieves 2.1μVrms noise in the integration bandwidth of 0.2 Hz–8 kHz with 7.7 μA total current in a die area of 355μm\times175μm in 180 nm CMOS technology. The presented design procedure is inherently technology agnostic. The novelty lies not in the architecture of the proposed neural amplifier, but in the proposed design procedure to optimise the noise-power-area trade-off in CMOS amplifier circuit design.</p>
28.	<p>Numerical Study of Droplets Coalescence in an Oil-Water Separator Z Hafsi, S Elaoud, M Mishra, I Wada - International Conference on Advances in Mechanical Engineering and Mechanics: Part of the Lecture Notes in Mechanical Engineering book series (LNME)</p> <p>Abstract: Through this paper a numerical modeling of oil-water flow through parallel plates integrated into a rectangular oil-water separator is conducted. Oil droplets of tiny sizes are dispersed in water and rectangular plates are used as coalescing chambers. Results have shown that upgrading a conventional API skimmer by introducing parallel coalescing chambers enhances coalescence of oil droplets by increasing their sizes. Since the buoyancy force that enables oil to float on water surface is proportional to the volume of the submerged oil droplet, droplets of greater sizes are then susceptible to rise to the water surface. Droplets floating on the water surface can be then easily skimmed. COMSOL Multiphysics modeling of two phase flow between two plates of the coalescing chamber has enabled to visualize the coalescence phenomenon and to determine coalesced droplets diameters. Further, the capability of enhancing oil water separation through coalescing chambers was discussed for the studied case.</p>
29.	<p>On bulk viscosity at weak and strong't Hooft couplings A Czajka, K Dasgupta, C Gale, S Jeon, A Misra... - Modern Physics Letters A, 2020</p> <p>Abstract: Bulk viscosity is an important transport coefficient that exists in the hydrodynamical limit only when the underlying theory is non-conformal. One example being thermal QCD with large number of colors. We study bulk viscosity in such a theory at low energies and at weak and strong 't Hooft couplings when the temperature is above the deconfinement temperature. The</p>

	<p>weak coupling analysis is based on Boltzmann equation from kinetic theory whereas the strong coupling analysis uses non-conformal holographic techniques from string and M-theories. Using these, many properties associated with bulk viscosity may be explicitly derived.</p>
30.	<p>Palladium-catalyzed regio- and stereoselective access to allyl ureas/carbamates: facile synthesis of imidazolidinones and oxazepinones IM Taily, D Saha, P Banerjee - <i>Organic & Biomolecular Chemistry</i>, 2020</p> <p>Abstract: Typically, transition metal catalysis enforces the stereodefined outcome of a reaction. Here we disclose the palladium-catalyzed regio- and stereoselective access to allylic ureas/carbamates and their further exploitation to diverse cyclic structures under operationally simple reaction conditions. This protocol features palladium-catalyzed decarboxylative amidation of highly modular VECs with good to excellent yield, minimal waste production, wide substrate scope, and low catalyst loading. In follow-up chemistry, we demonstrated the debenzoylation of vinylic imidazolidinones to N-hydroxycyclic ureas and regioselective derivatization towards the facile synthesis of halohydrins and oxiranes under mild reaction conditions in good to excellent yields.</p>
31.	<p>Pd Decorated Magnetic Spinels for Selective Catalytic Reduction of Furfural: Interplay of Framework Substituted Transition Metal and Solvent in Selective Reduction A Kumar, R Srivastava - <i>ACS Applied Energy Materials</i>, 2020</p> <p>Abstract: The reduction of functional platform chemicals, such as furfural, to industrially important chemicals and fuel, requires precise modulation of surface reactivity of the catalyst to obtain the desired reactivity and selectivity. In this study, the selective reduction of furfural (FAL) to furfuryl alcohol (FOL) and tetrahydrofurfuryl alcohol (THFA) is achieved by the transition metal interplay in the framework structure of magnetic spinels Fe₃O₄ and by modulating the reaction medium. Herein, FAL is selectively and quantitatively reduced to FOL in the water at very mild reaction conditions over Pd decorated CuFe₂O₄, whereas FAL is selectively converted to THFA in hexane at mild reaction conditions over Pd decorated NiFe₂O₄, using H₂ as an economical reducing agent. The Pd loading, reaction temperature, H₂ pressure, and reaction time are minimized to obtain the best selectivity towards THFA. Different modes of FAL adsorption occur on CuFe₂O₄ and NiFe₂O₄ surfaces. Dissociative adsorption of H₂ occurs on Pd sites to form Pd-H species, followed by the transfer hydrogenation from Pd-H to FAL adsorbed on spinels, leading to the formation of FOL or THFA. Efficient magnetic recyclability and hot filtration test shows that the catalyst exhibits no significant loss in the activity even after five cycles. Catalysts exhibit very high activity, selectivity, and low activation energy, which are very attractive for academic and industrial points of view.</p>
32.	<p>Power Consumption Analysis of Pulse Jet Filtration System Assisted with Pre-charger using Polyester Conductive Media S Dutta, A Mukhopadhyay, AK Choudhary, CC Reddy - <i>Journal of The Institution of Engineers (India): Series E</i>, 2020</p> <p>Abstract: Energy consumption is a vital aspect for any industry considering the cost-effective aspect. The current study embodies the power consumption during filtration of conductive filters at different dust pre-charging levels on laboratory-based pulse jet tubular set up assisted with pre-charger. Three types of polyester conductive non-woven filter materials, viz. PTFE-coated media, stainless steel fibre blended with PET media and stainless steel scrim media, have been characterized at three different charge levels, viz. 4 kV, 8 kV, 12 kV, and without charge. The outcome revealed that there has been a significant drop in power consumption with the rise in</p>

	<p>pre-charge level. Energy utilization results have further been compared with full-scale bag house condition by calculating the energy consumed for 50 bags. The results showed that among all the materials taken for investigation the performance of PTFE-coated media is the best and role of material is most significant towards the energy consumption by the filtration system. Overall energy consumption decreases with rise in pre-charging level. It is observed that percentage contribution of energy utilized for fan has been much higher for full-scale bag house as compared to tubular-based set-up. However, in case of energy consumed by the compressor, the difference in percentage contribution is relatively less and for energy utilized due to charge, not much variation in contribution can be noted.</p>
33.	<p>ReARM: A Reconfigurable Approximate Rounding-Based Multiplier for Image Processing R Bhattacharjya, A Kanani, N Goel - 24th International Symposium on VLSI Design and Test (VDAT), 2020</p> <p>Abstract: This paper aims to present a reconfigurable rounding based multiplier with different accuracy levels. It is based on a divide and conquer approach for applications in image processing. Our proposed approach divides the multiplicand and multiplier into two halves. Each half is multiplied with the other and our architecture is made accuracy-configurable. Further, due to rounding based approach, our approximate multiplication technique generates results faster. Based on our experiments, we observe that our proposed multiplier is 26.3% more accurate on an average compared to other state-of-the-art approximate multipliers for 8-bit operations.</p>
34.	<p>Reduplication initiated through discourse markers: A case of Hadoti G Chand, S Kar – Dialectologia, 2020</p> <p>Abstract: Reduplication is a common morphological process in many languages, particularly in South Asia. This study focuses on the reduplication phenomenon in Hadoti, where it ensues with the help of a discourse marker /rə/, functioning as an emphasizing agent in the process. This marker comes between the base and the reduplicant for expressing emphasis in work or action or verb (as in /k^ha rə k^ha/ ‘do eat,’ etc.). In Hadoti, /rə/ functions as a vocative case marker when it comes at the end of the sentence as in /ram gjo rə/ ‘Ram went’. However, when /rə/ occurs in between the base and the reduplicant, the stress shifts on the latter from the base. Phenomena of reduplication with a specific focus on the use of /rə/ are discussed in the current study using the constraints like *CLASH, and STRESS-TO-RED, etc. This particular phenomenon is predominantly present in the case of verbs in Hadoti, which is a unique feature of this variety of Hindi.</p>
35.	<p>Revisiting indeno [2, 1-c] fluorene synthesis while exploring the fully conjugated s-indaceno [2, 1-c: 6, 5-c'] difluorene H Sharma, PK Sharma, S Das - Chemical Communications, 2020</p> <p>Abstract: Described herein is an alternative synthetic approach for conjugated indeno[2,1-c]fluorene, including the experimental and theoretical investigations of a tetraradicaloid s-indaceno[2,1-c:6,5-c']difluorene that belongs to the rarely explored indacenodifluorene family containing $4n + 2$ monocyclic conjugated π-electrons. Expedient synthesis, broad absorption reaching 1150 nm, and small HOMO–LUMO energy gap make [2,1-c:6,5-c']s-IDF a promising candidate for optoelectronic applications.</p>

[Rotating five-dimensional electrically charged Bardeen regular black holes](#)
M Amir, MS Ali, SD Maharaj - Classical and Quantum Gravity, 2020

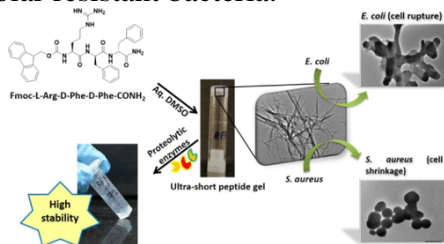
36.

Abstract: We derive a rotating counterpart of the five-dimensional electrically charged Bardeen regular black holes spacetime by employing the Giampieri algorithm on static one. The associated nonlinear electrodynamics source is computed in order to justify the rotating solution. We thoroughly discuss the energy conditions and the other properties of the rotating spacetime. The black hole thermodynamics of the rotating spacetime is also presented. In particular, the thermodynamic quantities such as the Hawking temperature and the heat capacity are calculated and plotted to see the thermal behavior. The Hawking temperature profile of the black hole implies that the regular black holes are thermally colder than its singular counterpart. On the other hand, we find that the heat capacity has two branches: the negative branch corresponds to the unstable phase and the positive branch corresponds to that of the stable phase for a suitable choice of the physical parameters characterizing the black holes.

[Self-Assembled Fmoc-Arg-Phe-Phe Peptide Gels with Highly Potent Bactericidal Activities](#)
N Chauhan, Y Singh - ACS Biomaterials Science & Engineering, 2020

37.

Abstract: The emergence of antibiotic resistance and the increasing rate of bacterial infections have motivated scientists to explore novel antibacterial materials and strategies to circumvent this challenge. Gels fabricated from ultrashort self-assembled peptides have turned out to be the most promising bactericidal materials. Self-assembled Fmoc-Phe-Phe gels have been extensively investigated earlier, and it has been shown that these gels possess potent bactericidal properties but suffer from disadvantages, such as poor proteolytic stabilities. In the present work, we report the highly potent bactericidal activities and proteolytic stability of gels fabricated from Fmoc-L-Arg-d-Phe-d-Phe-CONH₂ (RFF) peptide, which are best in class. We fabricated and characterized self-assembled gels (1–2% w/v) from Fmoc-d-Phe-d-Phe-CONH₂ (FF), Fmoc-L-His-d-Phe-d-Phe-CONH₂ (HFF), and Fmoc-L-Arg-d-Phe-d-Phe-CONH₂ (RFF) in aq dimethyl sulfoxide (35% v/v). The gels were characterized for their surface morphology, viscoelastic, self-healing, and stability characteristics. On incubation with proteolytic enzymes, FF gels did not show statistically significant degradation, and HFF and RFF gels showed only 43 and 32% degradation within 72 h at 37 °C, which is much better than gels reported earlier. The RFF gels (2%) exhibited more than 90% inhibition against Escherichia coli (Gram-negative) and Staphylococcus aureus (Gram-positive) within 6 h, and the activities were sustained for up to 72 h. The high-resolution transmission electron microscopy studies indicated electrostatic interactions between the gel and bacterial membrane components, leading to cell lysis and death, which was further confirmed by the bacterial cell Live/Dead assay. MTT assay showed that the gels were not toxic to mammalian cells (L929). The bactericidal characteristics of RFF gels have not been reported so far. The RFF gels show strong potential for treating device-related infections caused by antimicrobial-resistant bacteria.

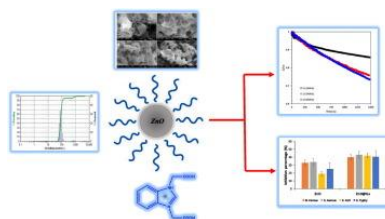


38.	<p>Solitons in a Spin-Orbit-Coupled Spin-1 Bose-Einstein Condensate S Gautam, SK Adhikari - <i>Brazilian Journal of Physics</i>, 2020</p> <p>Abstract: After the pioneering studies on spinor Bose-Einstein condensate (BEC) and after the realization of spin-orbit (SO) coupling in a spinor BEC of 87Rb and 23Na atoms, it is now realized that an SO-coupled BEC may reveal new physical phenomena not possible in a scalar BEC. For example, a new class of two- or three-dimensional vector soliton can be stabilized and observed in an SO-coupled BEC, whereas such a soliton is unstable in a scalar BEC. In this paper, we present a review on solitons in an SO-coupled spin-1 spinor BEC in one, two, and three space dimensions. In addition to the static properties of these solitons, we also consider their dynamics of motion with a constant velocity and collision between two solitons.</p>
39.	<p>Study of Mass-Asymmetric Fission of 180,190 Hg Formed in the 36 Ar+ 144,154 Sm Reactions D Kumar, EM Kozulin, M Cheralu, GN Knyazheva...PP Singh, RN Sahoo... - <i>Bulletin of the Russian Academy of Sciences: Physics</i>, 2020</p> <p>Abstract: t—The mass–energy distributions of fission fragments of excited $^{180,190}\text{Hg}$ nuclei formed in $^{36}\text{Ar} + ^{144,154}\text{Sm}$ reactions are measured at incident ^{36}Ar energies of 158, 181, and 222 MeV using the double-arm time-of-flight spectrometer CORSET. The asymmetric fission of $^{180,190}\text{Hg}$ with the most probable masses of light and heavy fragments of 79 and 101 amu, and 84 and 106 amu, respectively, is observed in mass distributions of $^{180,190}\text{Hg}$ at energies of excitation of up to 75 MeV. Two components manifesting the symmetric and asymmetric fission modes are observed in the kinetic energy distributions.</p>
40.	<p>Syllable structure and stratification in Bangla S Kar, H Truckenbrodt - <i>Journal of South Asian Languages and and Linguistics</i>, 2019</p> <p>Abstract: This study attempts to analyse the permissible syllable structures and the aspiration and voicing of word-initial and word-final segments in the syllable structure of Bangla. A corpus study leads to a detailed analysis of Bangla syllable structure restrictions, relative to the three traditional strata of the Bangla lexicon, namely, Native Bangla (NB, Tadbhava), Sanskrit borrowings (SB, Tatsama and Ardha-Tatsama), and other borrowings (OB, Deshi and Bideshi), following Ito and Mester’s work on the Japanese lexicon. Complex codas are allowed only in OB. Complex onsets are ruled out in NB while they have the maximal form s+C+liquid in SB and OB. There is no onset maximisation: Medial clusters in all strata avoid complex onsets if a consonant can be syllabified into the preceding coda (Vp.IV rather than V.plV). Aspiration is banned from the coda in NB but not generally in SB and OB, where restrictions that are more complex obtain. Obstruent voicing contrasts are present in onset and coda, but voicing agreement is enforced in obstruent clusters. Analyses of these restrictions are presented in Optimality Theory: the different strata of the lexicon may have different phonologies, i. e. different constraint ranking.</p>
41.	<p>Symmetry breaking by power-law coupling B Bandyopadhyay, T Khatun, PS Dutta... - <i>Solitons & Fractals</i>, 2020</p> <p>Abstract: We study the symmetry breaking phenomena in a network of Rayleigh oscillators coupled through power-law coupling whose interaction range is controlled by a power-law exponent. We show that in a broad range of the power-law exponent several symmetry-breaking states, such as amplitude chimeras and oscillation death are induced. Further, we observe an interesting transient behavior where amplitude chimeras and oscillation death states coexist. We establish the occurrence of the amplitude chimera using the theory of Floquet multipliers as well</p>

	<p>as other correlation measures. This paper deepens our understanding of the impact of power-law type interaction on symmetry-breaking states in a network of coupled oscillators.</p>
42.	<p>The influence of fibre alignment on the fracture toughness of anisotropic soft tissue A Baranwal, PK Agnihotri, JP McGarry - Engineering Fracture Mechanics, 2020</p> <p>Abstract: Finite element (FE) simulations are performed to investigate the effect of fiber induced anisotropy on the notch behavior in hyperelastic skin type materials. The modified anisotropic (MA) model is used to define the constitutive behavior in FE simulations through Abaqus user defined material model UMAT. A parametric study is carried out to examine the effect of fiber orientation, notch root radius and sample geometry on the stress field ahead of the notch tip. A non-dimensional parameter ξ is defined to characterize the combined effect of J energy and average anisotropic energy $\phi_{\text{aniso-avg}}$ on the notch behavior. It is shown that fibre orientation significantly influences the stress state and J-integral at the notch. The findings of the present study will be helpful in determining optimal constitution and orientation of skin grafts at locations of high stress and complex geometries, such as corner of eyes and lips, etc.</p>
43.	<p>Time-varying dependence between stock markets and oil prices during COVID-19: The case of net oil-exporting countries KP Prabheesh, B Garg, R Padhan - Economics Bulletin, 2020</p> <p>Abstract: This article provides an empirical investigation of the time-varying dependence between oil prices and stock markets in the top ten net oil-exporting countries. Using daily data focusing on COVID-19 period, we implement the DCC-GARCH to identify the dynamic dependence. Then, we apply structural break techniques to detect the shift in the dependence structure. We find that there exists a positive time-varying dependence between oil returns and stock returns during the ongoing COVID-19 pandemic wherein the breakpoints mostly coincided with the emergence of oil price war and global stock market crash. Overall, results imply that declining oil prices lead to a fall in stock returns due to lower future earnings for oil companies, exhibiting a signal of reduction in aggregate demand and economic activity in oil-exporting countries. Thus, the high positive co-movement may have ill-effects on portfolio diversification, as the latter will be less effective if the asset returns are highly correlated.</p>
44.	<p>Visible-Light Photoredox Catalyzed Recent Advances in the Utilization of CO₂ Feedstock for Organic Synthesis I Chatterjee, S Pradhan, S Roy, B Sahoo – Chemistry - A European Journal, 2020</p> <p>Abstract: CO₂ is a highly abundant, green and sustainable carbon-feedstock. Despite its kinetic inertness and thermodynamic stability, the development of various catalytic techniques has enabled the conversion of CO₂ to the value-added products such as carboxylic acids, amino acids and heterocyclic compounds, where visible light photocatalysis has emerged to be an efficient promoter of these processes. This minireview covers the progress in the areas of CO₂-incorporation onto organic matters based on the combined venture of renewable resources of CO₂ and light energy with significant emphasis on the last three years' development.</p>
45.	<p>Why ionic liquids coated ZnO nanocomposites emerging as environmental remediates: Enhanced photo-oxidation of 4-nitroaniline and encouraged antibacterial behavior LMG Rojas, CA Huerta-Aguilar... JS Sidhu, N Singh... - Journal of Molecular Liquids, 2020</p> <p>Abstract: In this paper, benzimidazole based ionic liquid (IL) was prepared, and then coated on ZnO to yield ZnO@IL which was then characterized systematically by different analytical methods such as X-Ray Diffraction (XRD), Scanning Electron Microscopy (SEM), and X-ray</p>

Photoelectron Spectroscopy (XPS) before exploring as a photo-catalyst for the oxidation of 4-nitroaniline (4-NA). In XRD, for ZnO@IL, the plane [100] has been shifted to higher angle at 64° in 2θ due to the influence of IL on the ZnO surface. The intensity and shape of the XPS peaks (appearing between 404 and 398 eV) originated from the IL's imidazole nitrogens indicate the existence of a sizable photoemission due to the interaction of NHCs with the electrophilic surface of ZnO. The catalytic oxidation of 4-NA (0.1 M) by ZnO@IL under UV light reveals a considerable degradation, which follows a first order kinetics. The formation of intermediates was analyzed by HPLC-MS, and proposed a possible mechanism for the oxidation. At low pH = 4, a greater oxidation rate ($k = 2.01 \times 10^{-4} \text{ mM}\cdot\text{s}^{-1}$) was obtained than that observed in higher pH of 10 ($k = 0.26 \times 10^{-4} \text{ mM}\cdot\text{s}^{-1}$). Additionally, ZnO@IL shows an antibacterial behavior exhibiting a significant microbial inhibition about 45%, and observed a considerable decrease in the cell growth if ZnO@IL presents in the culture medium.

Graphical Abstract:



Disclaimer: This publication digest may not contain all the papers published. Library has compiled the publication data as per the alerts received from Scopus and Google Scholar for the affiliation “Indian Institute of Technology Ropar” for the month of September 2020. The author(s) are requested to share their missing paper(s) details if any, for the inclusion in the next publication digest.